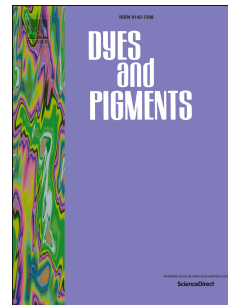


Accepted Manuscript

Studies of fluorine auxochrome in C9-fluorenyl anthracenes on optoelectronic property for blue electroluminescent materials

Guobin Ma, Huaxing Zhao, Jing Wang, Yuping Le, Haizhen Jiang, Hongmei Deng, Jian Hao, Wen Wan



PII: S0143-7208(18)30918-5

DOI: [10.1016/j.dyepig.2018.06.008](https://doi.org/10.1016/j.dyepig.2018.06.008)

Reference: DYPI 6813

To appear in: *Dyes and Pigments*

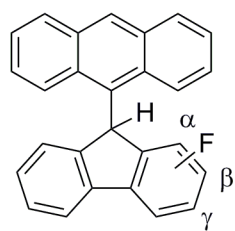
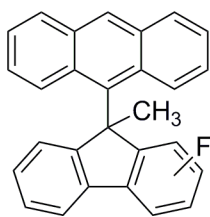
Received Date: 25 April 2018

Revised Date: 5 June 2018

Accepted Date: 6 June 2018

Please cite this article as: Ma G, Zhao H, Wang J, Le Y, Jiang H, Deng H, Hao J, Wan W, Studies of fluorine auxochrome in C9-fluorenyl anthracenes on optoelectronic property for blue electroluminescent materials, *Dyes and Pigments* (2018), doi: 10.1016/j.dyepig.2018.06.008.

This is a PDF file of an unedited manuscript that has been accepted for publication. As a service to our customers we are providing this early version of the manuscript. The manuscript will undergo copyediting, typesetting, and review of the resulting proof before it is published in its final form. Please note that during the production process errors may be discovered which could affect the content, and all legal disclaimers that apply to the journal pertain.

**3a-3c****4a-4c**

ACCEPTED MANUSCRIPT

Studies of fluorine auxochrome in C9-fluorenyl anthracenes on optoelectronic property for blue electroluminescent materials

Guobin Ma ^a, Huaxing Zhao ^{‡^a}, Jing Wang ^a, Yuping Le ^a, Haizhen Jiang ^a, Hongmei Deng ^b, Jian Hao ^{a, c, *}, Wen Wan ^{a, *}

^a Department of Chemistry, Shanghai University, Shanghai, 200444, China

^b Laboratory of Microstructures, Shanghai University, China

^c Key Laboratory of Organofluorine Chemistry, Shanghai Institute of Organic Chemistry, Chinese Academy of Sciences, Shanghai, China

* Corresponding author. Tel.: +81 21 66132190; fax: +81 21 66132190.

E-mail address: wanwen@staff.shu.edu.cn, jhao@shu.edu.cn

[‡] The author contributed equally to this work.

Abstract

Two series of fluorine-containing fluorenyl anthracenes linked by a rigid sp^3 -hybridized carbon atom have been synthesized and characterized. The effect of a fluorine auxochrome at different positions in fluorene moiety on bulk properties, such as photophysical, electrochemical properties and thermal stabilities were investigated. The non-doped organic light-emitting diodes (OLEDs) utilizing C9-methylated fluorinated fluorenyl anthracene **4b** as the emitter exhibits deep-blue emissions CIE x, y (0.159, 0.106) with efficiency of 1.31 cd/A and a maximum brightness of 2040 cd/m² at 14 V. It was found that the introduction of fluorine auxochrome to the C2 position of fluorene could afford the best performances of OLEDs among the fluorinated materials.

Keywords: Fluorenyl anthracenes, Twisted structure, Electroluminescence, Fluorine auxochrome, Blue OLED.

1. Introduction

In recent decades, great effort has been focused on the newly developed EL materials and the fabrication of organic light-emitting diodes due to their promising applications in full-color flat-panel displays and solid-state lighting [1-4]. Though a large number of EL materials have been synthesized and investigated, exploitation of new blue-emitting materials with high performance remains to be a great challenge. Compared with green and red light-emitting devices, the EL properties of blue-emitting devices still needs to be improved, particularly in terms of efficiency, color purity and lifetime for full-color applications [5-8]. Excellent blue-emitting materials are important, not only as blue emitters, but also as hosts for dopant emitters to facilitate efficient green and red emission.

Among the blue-emitting materials reported, fluorene and its derivatives are regarded as the most promising candidates for blue OLEDs, due to its attractive building block with high photoluminescence efficiency, high carrier mobility and easy modification [9-13]. In our previous work, a series of C-9 fluorene functionalized anthracene derivatives [14, 15], in which the anthracene and fluorene moieties were linked through a tetrahedral sp^3 -hybridized carbon atom, were studied. Similar to the spiro-annulated rigid molecule, the tetrahedral sp^3 -hybridized atom has presented an almost orthogonal linkage between the connected conjugated moieties. Due to its structural twisted configuration and non-planarity, the C-9 linked fluorene functionalized anthracene are expected to hinder close packing and intermolecular interactions, effectively minimize its degree of intermolecular stacking in the solid state, so that the tendency for molecules to crystallize should be reduced.

The fluorine atom is known as its strong electron-withdrawing ability and with isolated electron couple and fluorinated organic compounds play a key role in the remarkable progress of medicinal, agricultural, and material sciences [16-20]. Fluorination has been used in the past decade as a route to improve the electron transport in small molecules and polymer because of its strong electron-withdrawing ability [21-25]. Though fluorine containing materials used as light-emitting materials have been intensively studied in phosphorescent luminescent iridium (III) complexes [26-29], few examples of simple fluorine-containing organic compounds being directly

used as fluorescent luminescence materials were presented in reported articles [30-32].

In this work, we report the synthesis and luminescent properties of a series of fluorine containing fluorenyl-anthracene derivatives, in which the fluorine auxochrome was incorporated onto different positions of the fluorene moiety. The influences of fluorine auxochrome at the different position in the sterically twisted C9-fluorenyl anthracenes on optoelectronic property were elucidated for blue electroluminescent materials.

2. Experimental

2.1. Materials and measurements

All the reagents and solvents used for the syntheses and measurements were purchased from commercial suppliers and were used without further purification unless otherwise noted. The IR spectra were determined on a PE-1700 IR spectrophotometer by dispersing samples in KBr disks. ^1H , ^{13}C , ^{19}F NMR spectra were recorded on Bruker AV-500 spectrometer with CDCl_3 as deuterium solvent. High resolution mass spectra (HRMS) and Mass spectra (MS) were recorded using an Electron impact (EI) or Electrospray ionization (ESI) techniques. Elemental analyses were performed with Elemental Vario EL III instrument. UV-vis absorption spectra were recorded on CRAY-100 spectrophotometer. Fluorescence measurements were carried out with Perkin-Elmer LS55 in a solution of 10^{-6} mol/L and solid state, respectively. Oxidation-Reduction Potentials were measured using a Solartron SI 1287 electrochemical workstation (*vs* SCE). The melting points were measured by DSC on Netzsch STA409PC using a scanning rate of $10^\circ\text{C}/\text{min}$ with nitrogen flushing. The redox potentials of the compounds were determined with cyclic voltammetry (CV) using a Base 2000 CV system. HOMO values were recalculated from reported literature values as $\text{HOMO} = [E_{\text{onset}}]_{\text{red/ox}} (\text{vs SCE}) + 4.4$, $E_g = 1241/\text{UV}_{(\text{onset})}$. The luminance-Current-voltage characteristics were measured simultaneously by the programmable Keithley model 2400 and PR 650 spectrometer. All measurements were performed under an ambient atmosphere at room temperature.

2.2. Synthesis of 9-(1-fluoro-9H-fluoren-9-yl)anthracene (**3a**)

Anthracene (1.78 g, 10 mmol), zinc powder (0.65 g, 10 mmol), and 9-bromo-1-fluoro-

9H-fluorene (2.62 g, 10 mmol) were stirred in CS₂ (50 ml) and refluxed for 24 hours. After the reaction was cooled to room temperature and the solvent was removed by distillation, the residue was extracted with hot toluene and filtered to remove excess zinc. On cooling, a light yellow crystalline product was formed from the toluene solution, which was recrystallized from toluene again, and dried in a vacuum oven to obtain pale yellow crystal 2.3 g (64 %). M.p. 198-199 °C, ¹H NMR (500 MHz, CDCl₃): δ/ppm 8.68 (1H, d, *J*=9.0 Hz), 8.43 (1H, s), 8.08 (1H, d, *J*=8.0 Hz), 7.94 (1H, d, *J*=8.0 Hz), 7.88 (1H, d, *J*=8.5 Hz), 7.75(1H, d, *J*=7.5Hz), 7.61-7.58 (1H, m), 7.53-7.50 (1H, m), 7.41-7.37 (2H, m), 7.20-7.13 (2H, m), 7.03 (1H, d, *J*=7.5 Hz), 6.85-6.80 (2H, m), 6.74 (1H, d, *J*=9.0 Hz), 6.62(1H, s). ¹³C NMR (125 MHz, CDCl₃): δ/ppm 159.8 (¹*J*_{C-F}=247.5 Hz), 148.8, 143.8, 143.6, 139.6, 134.1, 131.9, 131.7, 130.4, 129.7 (³*J*_{C-F}=17.5 Hz), 129.3 (³*J*_{C-F}=17.5Hz), 129.1, 128.2 (²*J*_{C-F}=20.0 Hz), 127.4, 126.4, 125.3, 124.8, 120.8, 116.5 (⁴*J*_{C-F}=3.7 Hz), 114.4 (²*J*_{C-F}=20.0 Hz), 46.7 (³*J*_{C-F}=17.5 Hz). ¹⁹F NMR (470 MHz, CDCl₃): δ/ppm -118.00 (m). IR (KBr) ν_{max}/(cm⁻¹) 3042, 1934, 1621, 1473, 1445, 1342, 1286, 1159, 1018, 877, 783, 740, 727. HRMS (ESI-TOF): Found: [M+H]⁺ 361.1382; C₂₇H₁₈F requires [M+H]⁺ 361.1387. Elemental Anal. Calcd for C₂₇H₁₇F: C, 89.97; H, 4.75 %; Found: C, 89.93; H, 4.78 %.

Compounds **3b** and **3c** were synthesized according to the procedure described for **3a**.

2.3. Synthesis 9-(2-fluoro-9H-fluoren-9-yl)anthracene (**3b**)

Yield 53%. M.p 185-186 °C. ¹H NMR (500 MHz, CDCl₃): δ/ppm 8.64 (1H, d, *J*=4.5 Hz), 8.49 (1H, s), 8.14 (1H, dd, *J*=2.5 Hz), 7.95-7.91 (3H, m), 7.66-7.63(1H, m), 7.59-7.56 (1H, m), 7.43 (1H, t, *J*=7.5 Hz), 7.25-7.23 (1H, m), 7.17-7.14 (2H, m), 7.06 (1H, dd, *J*=7.5 Hz, *J*=2.5 Hz), 6.88-6.74 (1H, m), 6.69 (1H, dd, *J*=7.5 Hz, *J*=1.0 Hz), 6.64 (1H, d, *J*=1.0Hz), 6.49 (1H, s) ¹³C-NMR (125 MHz, CDCl₃): δ/ppm 162.9 (¹*J*_{C-F}=252.5 Hz), 151.2, 148.9, 139.4, 136.3 (⁴*J*_{C-F}=2.5Hz), 132.2, 131.8, 129.9, 129.0, 128.2, 127.3 (³*J*_{C-F}=12.5Hz), 126.7, 125.5, 124.9, 124.5, 123.7, 121.5 (³*J*_{C-F}=12.5 Hz), 120.2, 114.4 (²*J*_{C-F}=22.5 Hz), 112.0 (²*J*_{C-F}=22.5 Hz), 49.0. ¹⁹F-NMR (470 MHz, CDCl₃): δ/ppm -114.25 (m). IR(KBr) ν_{max}/(cm⁻¹) 3036, 1615, 1557, 1462, 1324, 1159, 1026, 973, 892, 730. HRMS (ESI-TOF): Found: [M+H]⁺ 361.1385; C₂₇H₁₈F requires [M+H]⁺ 361.1387. Elemental Anal. Calcd for C₂₇H₁₇F: C, 89.97; H 4.75 %; Found: C, 89.99; H, 4.77 %.

2.4. Synthesis of 9-(3-fluoro-9H-fluoren-9-yl)anthracene (**3c**)

Yield 62%. M.p. 177-178 °C. ¹H-NMR (500 MHz, CDCl₃): δ/ppm 8.53 (1H, d, *J*=8.5 Hz), 8.37 (1H, s), 8.02 (1H, d, *J*=7.5 Hz), 7.85 (1H, d, *J*=8.0 Hz), 7.80 (1H, d, *J*=8.0 Hz), 7.59 (1H, dd, *J*=9.0 Hz, *J*=2.5 Hz), 7.51-7.44 (2H, m), 7.35 (1H, t, *J*=7.5 Hz), 7.14-7.07 (2H, m), 6.99 (1H, dd, *J*=7.5 Hz, *J*=1.5 Hz), 6.89 (1H, dd, *J*=8.5 Hz, *J*=1.5 Hz), 6.80-6.74 (2H, m), 6.63 (1H, dd, *J*=9.0 Hz, *J*=2.5 Hz), 6.37 (1H, s). ¹³C-NMR (125 MHz, CDCl₃) δ/ppm = 162.8 (¹*J*_{C-F}=242.5 Hz), 149.9, 144.4 (⁴*J*_{C-F}=2.5 Hz), 142.1 (³*J*_{C-F}=8.7 Hz), 139.4 (⁴*J*_{C-F}=3.7 Hz), 132.2, 132.0, 131.1, 129.7, 129.5, 128.9, 128.0, 127.3, 126.6, 125.5 (³*J*_{C-F}=8.7 Hz), 124.8, 123.7, 120.8, 114.3 (²*J*_{C-F}=23.7 Hz), 107.6 (²*J*_{C-F}=23.7 Hz), 48.4. ¹⁹F-NMR (470 MHz, CDCl₃) δ/ppm = -115.34 (m). IR(KBr) ν_{max}/(cm⁻¹) = 3034, 1613, 1552, 1463, 1324, 1155, 1029, 978, 897, 736. HRMS (ESI-TOF): Found: [M+H]⁺ 361.1383; C₂₇H₁₈F requires [M+H]⁺ 361.1387. Elemental Anal. Calcd for C₂₇H₁₇F: C, 89.97; H, 4.75 %; Found: C, 89.92; H, 4.80 %.

2.5. Synthesis of 9-(1-fluoro-9-methyl-9H-fluoren-9-yl)anthracene (**4a**)

A solution of 9-(1-fluoro-9H-fluoren-9-yl) anthracene (720 mg, 2 mmol) in anhydrous THF (20 ml) was added with 1 ml of *n*-Butyl lithium (2.5 mmol 1.6 M) at 0 °C. After stirring for 3 hrs, 0.25 ml (4 mmol) of iodomethane was added to the reaction mixture and stirred for 2 hrs. Then, the reaction mixture was added to saturated ammonium chloride solution. The mixture was separated and extracted twice by 50 ml of ethyl acetate. The combined organic layer was washed with water, dried over magnesium sulfate and filtered. The solvent was removed and the residue was purified by recrystallization from dichloromethane and petroleum ether to afford white crystal 620 mg (83%). M.p. 194-195 °C. ¹H-NMR (500 MHz, CDCl₃): δ/ppm 8.28 (1H, s), 7.96 (1H, d, *J*=7.0 Hz), 7.90 (2H, t, *J*=8.0 Hz), 7.72 (1H, d, *J*=8.5 Hz), 7.63 (1H, dd, *J*=7.5 Hz, *J*=2.5 Hz), 7.50 (1H, dd, *J*=8.0 Hz, *J*=2.5 Hz), 7.32 (1H, t, *J*=8.0 Hz), 7.21 (3H, m), 7.12 (1H, dd, *J*=8.5 Hz, *J*=1.5 Hz), 7.07 (1H, t, *J*=8.0 Hz), 6.98 (1H, d, *J*=7.5 Hz), 6.90 (1H, dd, *J*=8.5 Hz, *J*=2.5 Hz), 6.73 (1H, dt, *J*=7.5 Hz, *J*=1.5 Hz), 1.84 (3H, s). ¹³C-NMR (125 MHz, CDCl₃): δ/ppm 162.8 (¹*J*_{C-F}=241.2 Hz), 155.7, 150.3 (⁴*J*_{C-F}=2.5 Hz), 141.3 (³*J*_{C-F}=8.7 Hz), 138.5, 134.1, 132.8, 130.9, 130.7, 129.2 (⁴*J*_{C-F}=3.7 Hz), 128.8, 128.6, 127.4 (³*J*_{C-F}=10.0 Hz), 127.2, 126.7, 125.4, 125.3 (³*J*_{C-F}=8.7 Hz), 124.9, 124.6, 124.5, 124.4, 124.3, 123.5, 120.9, 114.6 (²*J*_{C-F}=23.7 Hz), 107.6 (²*J*_{C-F}=23.7 Hz), 55.0, 30.9. ¹⁹F-NMR (470 MHz, CDCl₃): δ/ppm -115.39(m). IR(KBr) ν_{max}/(cm⁻¹) = 3032, 1616, 1560, 1460, 1328, 1159, 1028, 976, 898, 739. HRMS (ESI-TOF): Found: [M+H]⁺ 375.1540;

$C_{28}H_{20}F$: requires $[M+H]^+$ 375.1544. Elemental Anal. Calcd for $C_{28}H_{19}F$: C, 89.81; H, 5.11 %; Found: C, 89.85; H, 5.14 %.

Compounds **4b** and **4c** was synthesized according to the procedure described for **4a**

2.6. Synthesis of 9-(2-fluoro-9-methyl-9H-fluoren-9-yl)anthracene (**4b**)

Yield 67%. M.p. 194-195 °C. 1H -NMR (500 MHz, $CDCl_3$): δ /ppm 8.31 (1H, s), 8.05 (1H, d, $J=7.5$ Hz), 7.99 (1H, d $J=8.5$ Hz), 7.96-7.92 (2H, m), 7.81 (1H, d, $J=8.5$ Hz), 7.59-7.55 (1H, dd, $J=7.5$ Hz, $J=1.0$ Hz), 7.40-7.36 (1H, m), 7.31-7.28 (1H, m), 7.24 (1H, s), 7.19-7.18 (2H, m), 7.13-7.09 (2H, m), 7.07-7.04 (1H, m), 6.74 (1H, dd, $J=8.0$ Hz, $J=2.5$ Hz), 1.92(3H, s). ^{13}C -NMR (125 MHz, $CDCl_3$): δ /ppm 158.5 ($^1J_{C-F}=252.5$ Hz), 154.7, 138.5, 138.1, 135.3 ($^4J_{C-F}=2.5$ Hz), 132.8, 131.0, 130.6, 129.2 ($^3J_{C-F}=8.75$ Hz), 129.1, 128.7, 127.6, 127.4, 127.3, 126.7, 125.6, 125.4, 125.3, 124.8, 124.5 ($^3J_{C-F}=8.7$ Hz), 123.3, 121.7 ($^3J_{C-F}=8.7$ Hz), 121.6, 120.3, 114.5 ($^2J_{C-F}=22.5$ Hz), 110.9 ($^2J_{C-F}=23.7$ Hz), 55.5 ($^4J_{C-F}=1.2$ Hz), 30.8. ^{19}F -NMR (470 MHz, $CDCl_3$): δ /ppm -113.42 (m). IR(KBr) $\nu_{max}/(cm^{-1})$ 3034, 1620, 1562, 1460, 1324, 1159, 1029, 975, 897, 737. HRMS (ESI-TOF): Found: $[M+H]^+$ 375.1546; $C_{28}H_{20}F$: requires $[M+H]^+$ 375.1544. Elemental Anal. Calcd for $C_{28}H_{19}F$: C, 89.81; H, 5.11 %; Found: C, 89.77; H, 5.09 %.

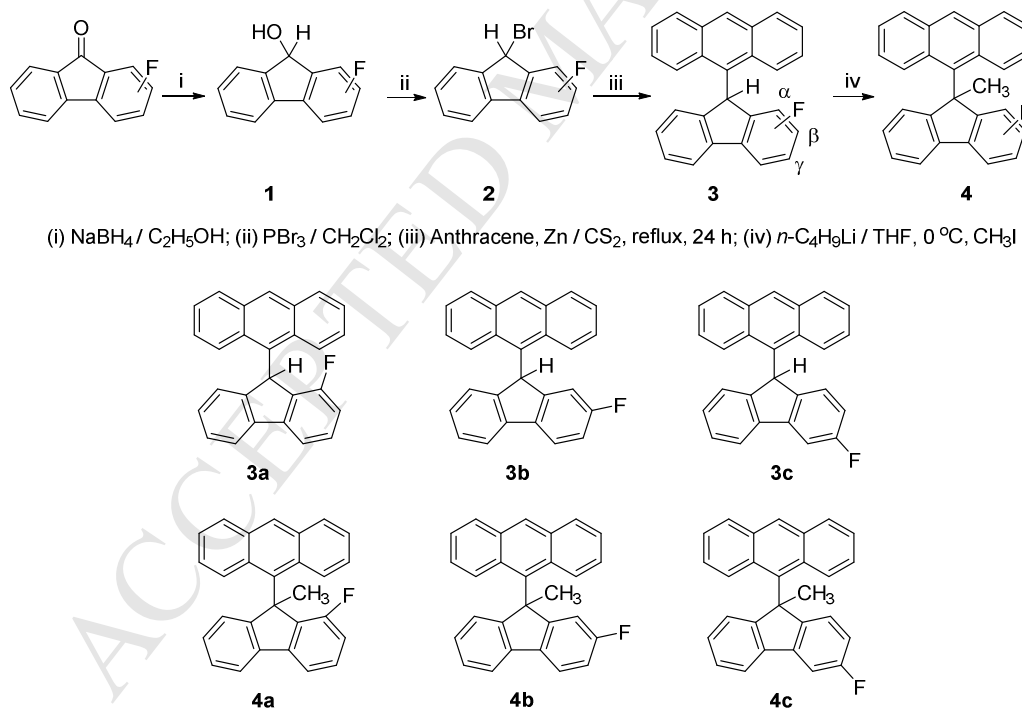
2.7. Synthesis of 9-(3-fluoro-9-methyl-9H-fluoren-9-yl)anthracene (**4c**)

Yield 78%. M.p. 165-166 °C. 1H -NMR (500 MHz, $CDCl_3$): δ /ppm 8.28 (1H, s), 7.96 (1H, d, $J=7.0$ Hz), 7.90 (2H, t, $J=8.0$ Hz), 7.72 (1H, d, $J=8.5$ Hz), 7.63 (1H, dd, $J=7.5$ Hz, $J=2.5$ Hz), 7.50 (1H, dd, $J=8.0$ Hz, $J=2.5$ Hz), 7.32 (1H, t, $J=8.0$ Hz), 7.21 (3H, m), 7.12 (1H, dd, $J=8.5$ Hz, $J=1.5$ Hz), 7.07 (1H, t, $J=8.0$ Hz), 6.98 (1H, d, $J=7.5$ Hz), 6.90 (1H, dd, $J=8.5$ Hz, $J=2.5$ Hz), 6.73 (1H, dt, $J=7.5$ Hz, $J=1.5$ Hz), 1.84 (3H, s). ^{13}C -NMR (125 MHz, $CDCl_3$): δ /ppm 162.8 ($^1J_{C-F}=241.2$ Hz), 155.7, 150.3 ($^4J_{C-F}=2.5$ Hz), 141.3 ($^3J_{C-F}=8.7$ Hz), 138.5, 134.1, 132.8, 130.9, 130.7, 129.2 ($^4J_{C-F}=3.7$ Hz), 128.8, 128.6, 127.4 ($^3J_{C-F}=10.0$ Hz), 127.2, 126.7, 125.4, 125.3 ($^3J_{C-F}=8.7$ Hz), 124.9, 124.6, 124.5, 124.4, 124.3, 123.5, 120.9, 114.6 ($^2J_{C-F}=23.7$ Hz), 107.6 ($^2J_{C-F}=23.7$ Hz), 55.0, 30.9. ^{19}F -NMR (470 MHz, $CDCl_3$) δ /ppm = -115.39(m). IR(KBr) $\nu_{max}/(cm^{-1})$ 3032, 1616, 1560, 1460, 1328, 1159, 1028, 976, 898, 739. HRMS (ESI-TOF): Found: $[M+H]^+$ 375.1542; $C_{28}H_{20}F$: requires $[M+H]^+$ 375.1544. Elemental Anal. Calcd for $C_{28}H_{19}F$: C, 89.81; H, 5.11 %; Found: C, 89.82; H, 5.13 %.

3. Results and Discussion

3.1. Synthesis of Fluorine-Containing Fluorenyl-Anthracene Derivatives

The main synthetic routes of the fluorine-containing blue light-emitting materials are shown in Scheme 1. Three Fluorine-containing 9-fluorenonees were synthesized from different starting materials through rationally designed ways with good yields and the experiment details were summarized in the supporting information for this article. Reduction of 9-fluorenonees with sodium borohydride in ethanol provided the fluorine-containing 9-hydroxyl fluorene derivatives **1a-1c**, which were further treated with phosphorus tribromide in methylene dichloride to give the corresponding 9-bromo fluorene derivatives **2a-2c**. Anthracene was refluxed with compounds **2a-2c** in the presence of zinc powder for 24 hours to generate **3a-3c** in modest yields (53%-64%). Finally, lithiation of compounds **3a-3c** with *n*-butyl lithium (*n*-BuLi) at 0 °C, followed by the treatment with iodomethane, gave the C-9 methylated compounds **4a-4c** in good yields (67-83%).



Scheme 1. Synthetic route towards fluorine-containing C-9 fluorene-functionalized anthracene derivatives

Thus, novel fluorine-containing fluorene-functionalized anthracene derivatives **3a-3c**, in which a rigid linkage of a tetrahedral *sp*³-hybridized carbon atom between fluorinated fluorene and

anthracene moieties (at the C-9 position of the fluorene) were prepared. In order to elevate rigidity, as well as electrochemical stabilities of these fluorine-containing fluorene-functionalized anthracenes, further methylation of compounds **3a-3c** at the active C9-H resulted the formation of C9-methylated anthracene derivative **4a-4c**, which were expected to exhibit stronger rigidity due to the existence of steric effect of methyl group. The chemical structures of **3a-3c** and **4a-4c** were confirmed by ^1H , ^{13}C , ^{19}F NMR and FT-IR spectroscopy. The results of the mass spectrometry and elemental analysis also supported the formation of the six blue emitting materials and matched well with the calculated data. Properties such as UV-vis absorption, photoluminescence, and electroluminescence including EL efficiency and color purity were evaluated. Compounds **3a-3c** and **4a-4c** have good solubility in common organic solvents so that they can be easily purified by column chromatography and recrystallization to high purity for spectroscopy characterization and OLEDs application.

3.3. Thermal Properties

Thermal properties of the six fluorine-containing C-9 fluorenyl-anthracene compounds **3a-3c** and **4a-4c** were investigated by thermogravimetric analysis (TGA) and differential scanning calorimetry (DSC) and summarized in Table 1. The Td is defined by a 5%-weight-loss temperature under a nitrogen atmosphere. It is found that the six compounds exhibit thermal stabilities with decomposition temperatures above 300 °C, as shown in the TGA measurements. Compounds **3a-3c** show a little higher thermal stability than those of the corresponding **4a-4c**, which indicate that the introduction of the methyl substituent at the C9-position of fluorene is unbeneficial for improving the morphological stability and resistance to the thermal decomposition. The tendency of both Td and Tm for **3a**>**3b**>**3c** and **4a**>**4b**>**4c** show that the closer position of fluorine atom to anthracene moiety would afford higher thermal stability.

3.4. Optical and Photoluminescent Characteristics

UV-vis absorption of each compound was tested in hexane, dichloromethane, chloroform, ethylacetate, tetrahydrofuran and ethanol, respectively, to investigate the solvent effects. All compounds exhibit the characteristic vibrational patterns of isolated anthracene group with three strong absorption bands in the region of 340-420 nm, indicating the existence of a π - π^* transition

derived from the substituted anthracene backbone. Only 1~4 nm shift based on different solvents are observed (seen Fig.S7-Fig.S12 in SI). A comparison of the absorptions in dichloromethane solution in Fig. 1 demonstrate that compounds **3a-3c** give nearly the same vibronic patterns at 350 nm, 369 nm and 389 nm, while C9-methylated compounds **4a-4c** provide the peak wavelength around 343 nm, 363 nm and 381 nm. These results indicate that the fluorine auxochrome at different position on the fluorene moiety in compounds **3a-3c** exhibit much less influence on Uv-vis absorption than those of C9- methylated analogues. A blue shift of less than 10 nm is presented in the absorption spectra of C9- methylated **4a-4c**. Compounds **4a-4c** show bigger UV band edge than **3a-3c**, suggesting that the C9-methylated compounds would have larger energy gap.

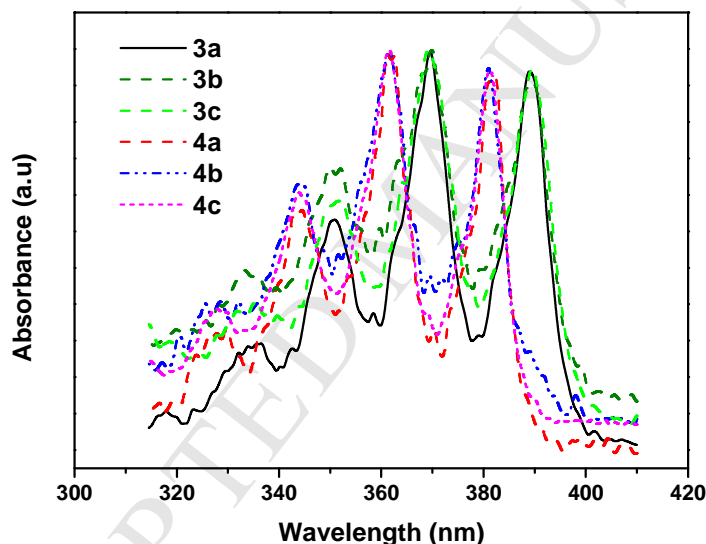


Figure 1. UV-vis absorption of compounds **3a-3c** and **4a-4c** in CH_2Cl_2 solution (1×10^{-6} M)

The photoluminescence of each compound was also measured in hexane, dichloromethane, chloroform, ethyl acetate, tetrahydrofuran and ethanol, respectively, to investigate the influence of solvents (Seen Fig.S13-Fig.S18 in SI). Shifts of less than 4 nm are observed for three main emission around 390 nm, 415 nm and 445 nm, which are similar to the emission peaks of anthracene. Fig. 2 (a) and Fig. 2 (b) show the photoluminescence of all compounds in dichloromethane solution and solid state at room temperature, respectively. The PL spectra of compounds **3a-3c** in solution from Fig. 2(a) present almost identical fluorescent emission pattern

with three emission peaks at 394 nm, 418 nm and 444 nm, only 1 nm shift difference for each compound **3a-3c** with fluorine-containing group at different substituted position. Compared with the analogues of compounds **3a-3c**, a blue shift of around 10 nm is detected on PL spectra of emission peaks located around 384 nm, 408 nm and 431 nm for compounds **4a-4c**.

The PL spectra in solid states shown in Fig. 2(b) for all synthesized compounds exhibit a maxima emission peak in the blue region of 420-450 nm, which have red shift about 10 nm in comparison with those in dilute solution. The bathochromic shift on the fluorescent emissions is probably due to the difference in dielectric constant of the environment. The PL spectra for **4a** and **4b** showed 2-3 nm red shift, compared with that of **4c**. The PL spectra in solid states for compounds **4a-4c** show almost the same spectra around 420 nm and 440 nm, suggesting that the intermolecular interactions are restrained effectively by the twisted bulky fluorenyl-anthracene units after methylation of C9-H in compounds **3a-3c**. These phenomena of PL in solid state are also observed by careful studies between compounds **3a**, **3b**, which reveal that the fluorine auxochrome at the 1- or 2-position of fluorene moiety cause little effect on the emission process. However, the PL spectra around 430 nm and 451 nm for **3c**, which has a fluorine substituent at the 3-position of fluorene, presents a stronger bathochromic effect with the respect of **3a** and **3b** with fluorine atom at 1- or 2-position. The fluorescence quantum yield was measured by calibrating against quinine sulfate ($\phi_f \approx 0.55$) [33]. The emission quantum yields are high in the region of 0.79-0.92, indicating that these fluorine containing compounds would have good efficient electroluminescent properties in OLED devices.

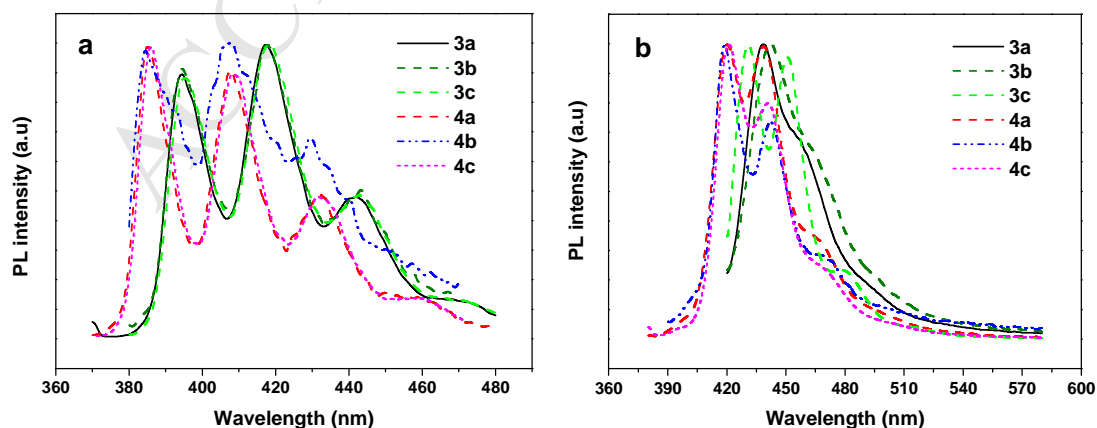


Figure 2. Photoluminescence in dichloromethane solvent (a) (1×10^{-6} M) and in solid states (b)

3.5. Electrochemical Behavior

To explore the influence of chemical structure on the electrochemical properties of these materials, the redox potentials of the compounds were determined with cyclic voltammetry (CV) measurements, which were carried out in a three-electrode cell setup with 0.1 M tetrabutyl-ammonium hexafluorophosphate (Bu_4NPF_6) as a supporting electrolyte in anhydrous CH_2Cl_2 to probe the electrochemical behavior of the materials. The molecular orbital energy levels of compounds **3a-3c** and **4a-4c** have been derived from cyclic voltammetry (CV) (Fig. 3) in combination with the optical band gaps (E_g) determined by the onset of the absorption in solution and are presented in Table 1.

HOMO values were calculated from $\text{HOMO} = [E_{\text{onset}}]_{\text{red/ox}} (\text{vs SCE}) + 4.4$, $E_g = 1240 / \text{UV}(\text{onset})$ [34]. All compounds show a reversible oxidation process, indicating their electrochemical stabilities. As seen from Fig. 3 and Table 1, all HOMO energies of the fluorine-containing fluorenyl-anthracene derivatives are at about 5.62 - 5.70 eV. Such a low HOMO energy level greatly reduces the energy barrier for hole injection from indium tin oxide (ITO) to the emissive fluorine-containing anthracene-fluorene derivatives. The energy band gaps (E_g), which are estimated from the onset of the absorption spectra, are located around 3.10 eV for compounds **3a-3c** and 3.15 eV for compounds **4a-4c**, respectively, suggesting that these newly prepared compounds are potentially suitable as blue emitting materials. A larger energy gap (E_g) for **4a-4c** than those of **3a-3c** would be resulted from the distorted π -conjugation on the fluorenyl anthracene molecule due to the replacement of C9-H with the bulky methyl group. The LUMO energies are calculated around 2.5 eV-2.6 eV by combining the HOMO energy levels together with the bandgaps obtained from the absorption edge. Compared with the analogues of compound **3a-3c**, compounds **4a-4c** show relatively lower HOMOs and LUMOs energies with larger bandgaps (E_g). The substitution position of the fluorine atom on fluorene moiety doesn't show considerable difference on molecular orbital energy on the series **3** and **4**. The energy gap for these compounds are found to show little relationship with the substituted position of fluorine atom on fluorine moiety.

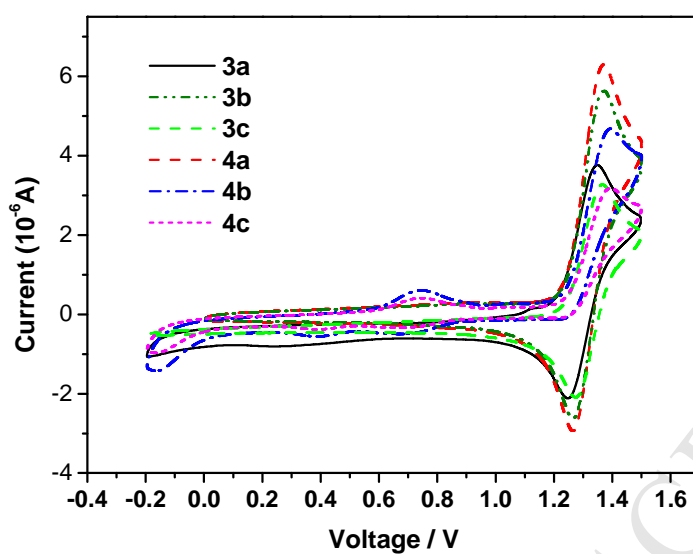


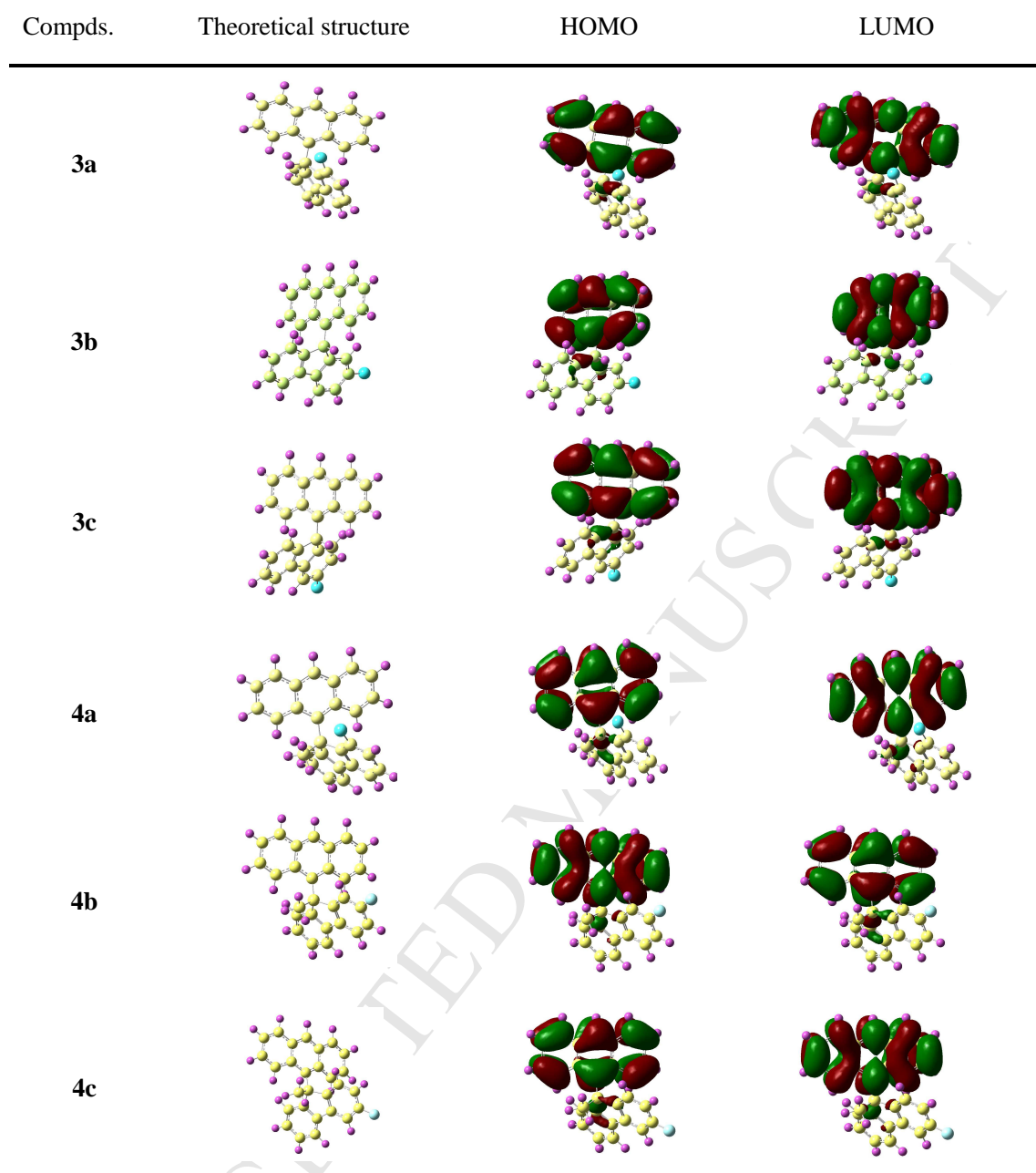
Figure 3. The curves of cyclic voltammetry for the fluorine-containing compounds **3a-3c** and **4a-4c**

Table 1. Optical, thermal and electrical properties of compounds

Compd.	$\lambda_{\text{max, Abs}}$ (nm) ^a	$\lambda_{\text{max, PL}}$ (nm) ^a	$\lambda_{\text{max, PL}}$ (nm) ^b	QE (ϕ) ^c	$E_{1/2}$ (eV)	HOMO (eV)	LUMO (eV)	E_g (eV)	T_d (°C)	T_m (°C) ^d
3a	350, 369, 389	394, 417, 442	439	0.79	1.29	5.69	2.61	3.08	385	198
3b	351, 370, 390	395, 418, 443	440	0.82	1.31	5.70	2.60	3.10	355	185
3c	352, 369, 389	394, 418, 442	430, 451	0.86	1.31	5.70	2.60	3.10	332	177
4a	343, 362, 381	384, 407, 430	420, 442	0.89	1.23	5.62	2.47	3.15	339	194
4b	344, 363, 382	385, 408, 431	420, 443	0.92	1.22	5.63	2.49	3.14	312	183
4c	343, 362, 381	384, 408, 430	419, 440	0.84	1.23	5.63	2.49	3.14	308	165

^a Measured in CH₂Cl₂ solution. ^b Film samples. ^c Fluorescence quantum efficiency, relative to quinine sulfate in cyclohexane ($\phi_f \approx 0.55$). ^d Melting point

Three-dimensional geometries and the frontier molecular orbital energy levels of compounds **3a-3c** and **4a-4c** were accomplished using density functional theory (DFT) calculations at the B3LYP/6-31G* level on Gaussian 03 programs [35-37]. Their ground geometries and the orbital plots of the HOMO-LOMOs were illustrated in Figure 4. Obviously, they exhibit large torsion angles in the optimized geometries. The calculated geometries and that comparison with X-ray diffraction analysis of the known fluorine-free analogue [14, 15] demonstrate that the fluorine-containing fluorene and the anthracene moieties are significantly twisted against each other through the linkage of the sp^3 -hybridized carbon atom, resulting in a non-coplanar twisted conformation in each molecule. Due to the introduction of the bulky methyl group, compound **4a-4c** exhibit an almost orthogonal conformation. These dramatically twisted conformations can effectively prevent intermolecular interactions between π -systems of aromatic rings, which are proposed to suppress the crystallization of the materials and finally improve the morphological stability of these molecules. Such a unique twisted structural feature of fluorenyl-anthracene is beneficial for their suppressing on fluorescent quenching induced by the aggregation in the solid states and for the formation of uniform amorphous morphology in the film state of OLED device. The calculated electron densities of the HOMOs and LUMOs are mainly localized on the anthracene moiety, indicating that the absorption and emission process are only attributed to the π - π^* transition centered on the anthracene moiety. Thus, the excellent luminescence efficiency of anthracene moiety in the synthesized compounds can be maintained.

Figure 4. HOMO and LUMO electronic density distributions of **3a-3c** and **4a-4c**

3.6. OLED Fabrication

To investigate their potential applications in OLED, these fluorine-containing fluorenyl anthracene derivatives **3a-3c** and **4a-4c** were used as emitting layer by thermal evaporation technique with following configuration to fabricate simple non-doped OLED devices. The device structure is depicted in Figure 5 (a): ITO/MoO_x (4 nm)/NPB (20 nm)

/Emitting layer(30 nm) /Bphen (20 nm) /LiF (0.7 nm)/Al, where *N*, *N'*-diphenyl-*N*, *N'*-bis(1-naphthyl)-(1,1-biphenyl)-4,4'-diamine (NPB), 4,7-diphenyl-1,10- phenanthroline (Bphen) were used as hole-transporting and electron-transporting layer, respectively. The combination of a thin LiF layer and Al were applied to form an efficient cathode and ITO (indium tin oxide) was used as anode. The ITO glass substrate was cleaned with detergent and deionized water and dried in an oven. It was then treated with UV-ozone for 30 minutes before loading into a deposition chamber. The organic films of NPB, emitting material, Bphen and LiF/Al were sequentially deposited onto the ITO substrate at a pressure of around 3×10^{-4} Pa. The EL spectra and luminance were recorded on a PR650 spectrometer. Luminance-voltage and current-voltage characteristics were measured at room temperature.

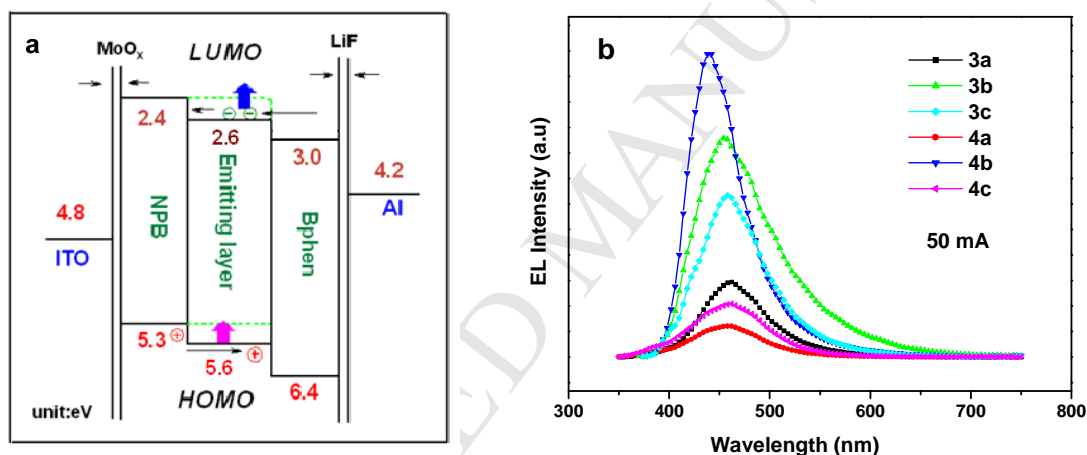


Figure 5. Schematic energy level of different layer (a) and EL spectra of six fluorine- containing fluorenyl-anthracene derivatives at 50 mA (b)

As shown in the schematic energy level diagram of OLEDs in Fig.5 (a), the hole-injection barrier at NPB/emitter is about 0.3 V, while the electron-injection barrier at the emitter is about 0.4 V. These small injection barriers could enhance the efficient injection of both holes and electrons into the emission layer. Fig. 5 (b) shows the typical EL spectra of OLEDs based on **3a-3c** and **4a-4c** as the emitting layers, suggesting that carriers recombination is effectively restricted in these blue materials when compared with their PL ones. All devices exhibit blue emission with peak maxima between 444-468 nm. A stable emission in EL spectra and CIE coordinates from all

diodes obtained on different applied voltages demonstrate that these fluorine-containing compounds reveal excellent operating stabilities for blue emission. In comparison with the corresponding PL of solid states, the EL spectra for compounds **3a-3c** and **4a-4c** are found to afford a red shift of about 20 nm, which may be caused by the intermolecular interactions and the electrical field polarization in the excited states. Compound **3a** shows the emission peak at 468 nm with a width at half maximum (FWHM) about 80 nm and compounds **3b**, **3c** afford the emission peak at 464 nm with a width at half maximum (FWHM) about 70 nm, giving only 4 nm blue shift difference according to the study on the influence of different fluorine substituted positions. While, compound **4a** provides the emission peak at 468 nm with a FWHM about 80 nm and compound **4c** gives the emission peak at 462 nm with a FWHM about 70 nm, respectively. It is interesting to find that compound **4b**, which has a fluorine substituent at the 2-position on the fluorene moiety of C9-methylated fluorene-anthracene derivative, exhibits the emission peak at 444 nm with the narrowest FWHM around 60 nm among all the derivatives, giving nearly 20 nm blue shift in comparison with **3b** or **4a**. Those results indicate that the incorporation of a fluorine atom into the C2-position of the fluorene moiety in the methylated fluorene-anthracene would have significant steric hindrance and greatly reduce the aggregation formation emitting at longer wavelengths [38, 39].

The EL performance of the six devices is studied in Figure 6, and the key parameters are collected in Table 2.

The devices based on compounds **3a**, **3b** and **4a** show a sky-blue emission with CIE coordinates for **3a** (0.169, 0.313), **3b** (0.168, 0.230), **4a** (0.157, 0.272), while a deep-blue emission for devices from **3c** (0.160, 0.165), **4c** (0.162, 0.122), especially that for compound **4b** (0.159, 0.106), which is very close to the pure blue light (0.159, 0.080) presented. However, it is found that compounds **3a**, **3b** and **4a** exhibit CIE coordinates of $y > 0.23$ with an obvious observation of red shift of emission peak and wider FWHM. By analysis of the coordinates of compounds **3a**, **3b** and **3c**, it can be clearly observed that incorporation of a fluorine atom further away from the anthracene moiety would provide deeper blue (smaller y coordinates) emission. Interestingly, compound **4b** is endowed with significant deep-blue emission among **4a-4c**. This might be ascribed to the collaborative effect for an isolated electron couple, electron-withdrawing ability of

fluorine atom and the steric effect of C9 methyl group.

As shown by the voltage-current density-luminance characteristics (Fig. 6 (a) and Fig. 6(b)) and the efficiency curves (Fig.6 (c)), the devices based on the blue emitters **3a-3c** exhibit a maximum current efficiency of 1.01 cd/A, 1.06 cd/A and 1.17 cd/A with a maximum brightness of 1219 cd/m², 1808 cd/m² and 1826 cd/m² at 14 V, respectively. However, much-higher EL efficiencies are obtained with a maximum current efficiency of 1.46 cd/A, 1.31 cd/A, 1.27 cd/A and a maximum brightness of 2070 cd/m², 2040 cd/m², 1795 cd/m² for **4a**, **4b** and **4c** at 12V, respectively. It is interesting to find that a better luminescence efficiency would be obtained when the fluorine substituent is positioned away from anthracene moiety in compound **3a-3c**. In contrast, an opposite trend of luminescence efficiency would be observed in the case of C9-methylated fluorenyl-anthracene **4a-4c**. It is obvious that the current density and maximum brightness for **4b**-based device provided the best performance among these of the corresponding devices, despite the identical device configuration applied. As it is known that the fluorine atom exhibits very strong electron-withdrawing ability and the possible interaction of fluorine atom with the adjacent aromatic-H, compound **4b** would probably present the most suitable electric and steric effect among the prepared C9-methylated fluorinated fluorenyl anthracene, due to the incorporation of the fluorine atom into the 2-position on fluorenyl moiety. The steric and electronic configuration of **4b** would contribute to the best performance among **4a-4c**. It is also found from Fig. 6 (c) that the efficiencies for these fluorine-containing derivatives have only a mild decrease as the current density increase. The devices based on **4a-4c** provide better luminous efficiencies than those for the counterpart **3a-3c**, indicating that the highly twisted structure and strong rigidity of the fluorine-containing fluorenyl-anthracene molecules induced by the steric effect of the methyl group would play an important role in the improvement of the luminous efficiency. Additionally, all devices have turn-on voltages of 4.2-5.1 V at a brightness of 1 cd/m². One important reason for such similar turn-on voltages is that the injection barriers in the devices are very close to each other.

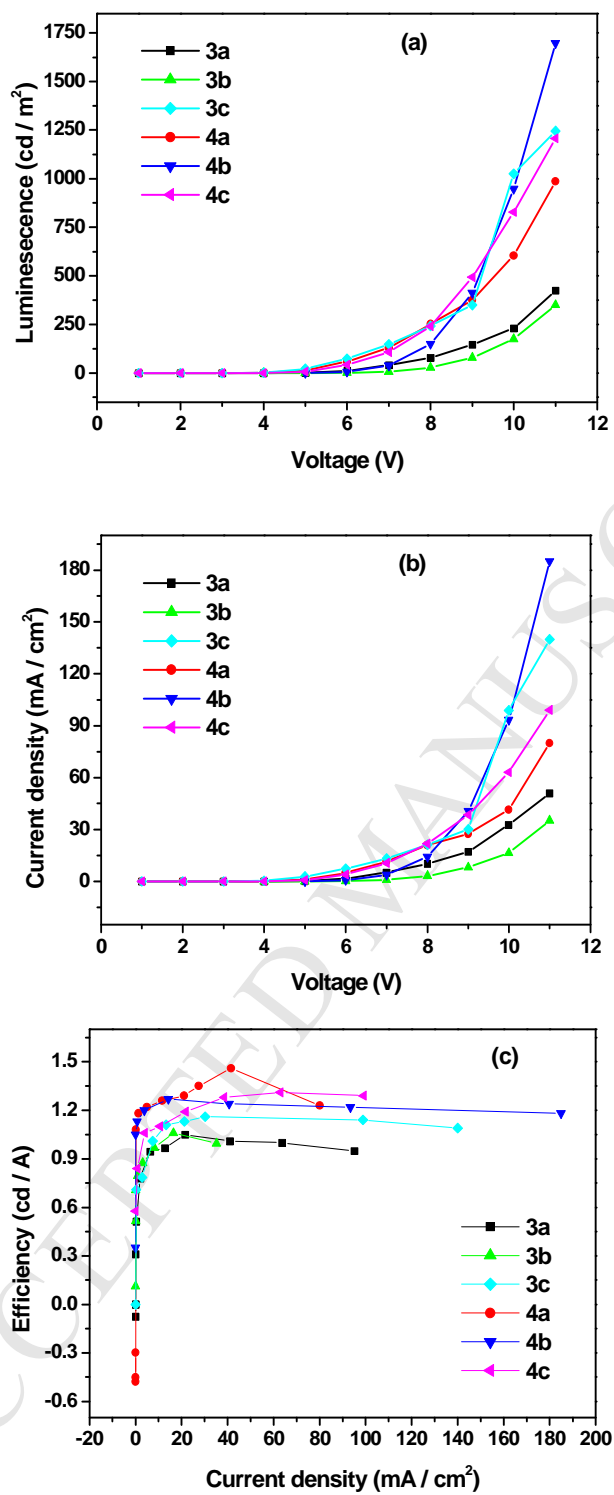


Figure 6. Luminescence-Voltage (V) (a), Current density (I)-voltage (V) (b) and L-C (luminance efficiency vs.

current density) characteristics (c) for the six fluorine- containing fluorenyl- anthracene derivatives

Table 2. Electroluminescence properties of compounds

Compd.	EL _{max} (nm)	Brightness (cd/m ²)	Efficiency (cd /A)	CIE (x, y)
3a	468	1219 ^a	1.01	0.169, 0.313
3b	464	1808 ^a	1.06	0.168, 0.230
3c	464	1826 ^a	1.17	0.160, 0.165
4a	468	2070 ^b	1.46	0.157, 0.272
4b	444	2040 ^b	1.31	0.159, 0.106
4c	462	1795 ^b	1.27	0.162, 0.122

^a the data were measured at 14 V, b: the data were obtained at 12 V

Conclusion

In summary, six fluorinated fluorenyl functionalized anthracenes, which contain a twisted configuration due to the rigid linkage of a sp^3 -hybridized carbon atom were prepared and described. The DFT theoretical calculation supports that the synthesized materials have non-coplanar structures with large intramolecular torsion angles, which would avoid π - π stacking in the solid state. The experimental results were well supported by DFT theoretical calculations. The compounds **3a-3c** and **4a-4c** exhibit strong blue PL emissions, good thermal stability, and good film forming property. The effects of the fluorine auxochrome at the substituted position of the fluorene moiety on the photophysical, electrochemical properties and thermal stabilities, as well as the performance of non-doped blue-light-emitting OLED have been discussed. The introduction of fluorine atom into fluorenyl functionalized anthracene at C2-position (**4b**) could give the excellent electroluminescent performance among the host emitter materials synthesized in this work.

Acknowledgements

This work was financially supported by the National Natural Science Foundation of China (No. 21572128, 21672139) and the Science Foundation of Shanghai Municipal Commission of Sciences and Technology (No. 15230724800). The authors thank the Laboratory of

Micro-structures of Shanghai University for structure analysis.

References:

- [1] Baldo M, Lamansky S, Burrows P, Thompson M, Forrest S. Very high-efficiency green organic light-emitting devices based on electrophosphorescence. *Appl Phys Lett* 1999; 75: 4-6.
- [2] Yang X, Xu X, Zhou G. Recent advances of the emitters for high performance deep-blue organic light-emitting diodes. *J Mater Chem* 2015; 3: 913-44.
- [3] Kim J, Liu M, Jen A. Bright red-emitting electrophosphorescent device using osmium complex as a triplet emitter. *Appl Phys Lett* 2003; 83: 776-8.
- [4] Carlson B, Phelan G, Kaminsky W, Dalton L, Jiang X, Liu S, Jen A. Divalent osmium complexes: synthesis, characterization, strong red phosphorescence, and electrophosphorescence. *J Am Chem Soc* 2002; 124: 14162-72.
- [5] Zhang S, Yao L, Peng Q, Li W, Pan Y, Xiao R, Gao Y, Gu C, Wang Z, Lu P, Li F, Su S, Yang B, Ma Y. Achieving a significantly increased efficiency in nondoped pure blue fluorescent OLED: a quasi-equivalent hybridized excited state. *Adv Funct Mater* 2015; 25: 1755-62.
- [6] Shi L, Liu Z, Dong G, Duan L, Qiu Y, Jia J, Guo W, Zhao D, Cui D, Tao X. Synthesis, structure, properties, and application of a carbazole-based diaza[7]helicene in a deep-blue-emitting OLED. *Chem Eur J* 2012; 18: 8092-99.
- [7] Lee S, Kim B, Jung H, Shin H, Lee H, Lee J, Park J. Synthesis and electroluminescence properties of new blue dual-core OLED emitters using bulky side chromophores. *Dyes Pigments* 2017; 136: 255-61.
- [8] Shih P, Chuang C, Chien C, Diao E, Shu C. Highly efficient non-doped blue-light-emitting

- diodes based on an anthracene derivative end-capped with tetraphenylethylene groups. *Adv Funct Mater* 2007; 17: 3141-6.
- [9] Wong K, Chien Y, Chen R, Wang C, Lin Y, Chiang H, Hsieh P, Wu C, Chou C, Su Y, Lee G, Peng S. Ter(9,9-diarylfluorene)s: Highly efficient blue emitter with promising electrochemical and thermal stability. *J Am Chem Soc* 2002; 124: 11576-7.
- [10] Saragi T, Spehr T, Siebert A, Fuhrmann-Lieker T, Salbeck J. Spiro compounds for organic optoelectronics. *Chem Rev* 2007; 107: 1011-65.
- [11] Luo J, Zhou Y, Niu Z, Zhou Q, Ma Y, Pei J. Three-dimensional architectures for highly stable pure blue emission. *J Am Chem Soc* 2007; 129: 11314-5.
- [12] Wong K, Wang Z, Chien Y, Wang C. Synthesis and properties of 9,9-diarylfluorene-based triaryldiamines. *Org Lett* 2001; 3: 2285-88.
- [13] Feng X, Chen S, Ni Y, Wong M, Maggie. Lam M, Cheah K, G Lai, Fluorene derivatives for highly efficient non-doped single-layer blue organic light-emitting diodes. *Org Electron* 2014; 15: 57-64.
- [14] Wang J, Wan W, Jiang H, Gao Y, Jiang X, Lin H, Zhao W, Hao J. C-9 Fluorenyl substituted anthracenes: a promising new family of blue luminescent materials. *Org Lett* 2010; 12: 874-7.
- [15] Wan W, Du H, Wang J, Le Y, Jiang H, Chen H, Zhu S, Hao J. Novel blue luminescent materials for organic light-emitting diodes based on C9-fluorenyl anthracenes. *Dyes Pigments* 2013; 96: 642-52.
- [16] Banks R, Smart B, Tatlow J. *Organofluorine chemistry: principles and commercial applications*; Plenum Press: New York, 2000.

- [17] Hiyama T, Kanie K, Kusumoto T, Morizawa Y, Shimizu M. Organofluorine compounds: chemistry and application; Springer-Verlag: Berlin, 2000.
- [18] Kirsch P. Modern Fluoroorganic chemistry; Wiley-VCH: Weinheim, 2004.
- [19] Chambers R. Fluorine in organic chemistry; Blackwell: Oxford, 2004.
- [20] Wan W, Ma G, Li J, Chen Y, Hu Q, Li M, Jiang H, Deng H, Hao J. Silver-catalyzed oxidative decarboxylation of difluoroacetates: efficient access to C-CF₂ bond formation. Chem Commun 2016; 52: 1598-61.
- [21] Reddy J, Kale T, Balaji G, Chandrasekaran A, Thayumanavan S. Cyclopentadithiophene-based organic semiconductors: effect of fluorinated substituents on electrochemical and charge transport properties. J Phys Chem Lett 2011; 2: 648-54.
- [22] Crouch D, Skabara P, Lohr J, McDouall J, Heeney M, McCulloch I, Sparrowe D, Shkunov M, Coles S, Horton P, Hursthouse M. Thiophene and selenophene copolymers incorporating fluorinated phenylene units in the main chain: synthesis, characterization, and application in organic field-effect transistors. Chem Mater 2005; 17: 6567-78.
- [23] Facchetti A, Yoon M, Stern C, Katz H, Marks T. Building blocks for n-type organic electronics: regiochemically modulated inversion of majority carrier sign in perfluoroarene-modified polythiophene semiconductors. Angew Chem Int Ed 2003; 42: 3900-03.
- [24] Crouch D, Skabara P, Heeney M, McCulloch I, Coles S, Hursthouse M. Hexyl-substituted oligothiophenes with a central tetrafluorophenylene unit: crystal engineering of planar structures for p-type organic semiconductors. Chem Commun 2005; 1465-67.
- [25] Tang M, Bao Z. Halogenated materials as organic semiconductors. Chem Mater 2011; 23:

446-55.

- [26] Cornil J, Gruhn N, Dos Santos D, Malagoli M, Lee P, Barlow S, Thayumanavan S, Marder S, Armstrong N, Bédas J. Joint experimental and theoretical characterization of the electronic structure of 4,4'-bis(N-m-tolyl-N-phenylamino)biphenyl (TPD) and substituted derivatives. *J Phys Chem A* 2001; 105: 5206-11.
- [27] Kessler F, Watanabe Y, Sasabe Y, Katagiri H, Nazeeruddin M, Grätzel M, Kido J. High-performance pure blue phosphorescent OLED using a novel bis-heteroleptic iridium(III) complex with fluorinated bipyridyl ligands. *J Mater Chem* 2013; 1: 1070-75.
- [28] Shao S, Ding J, Wang L, Jing X, Wang F. White electroluminescence from all-phosphorescent single polymers on a fluorinated poly(arylene ether phosphine oxide) backbone simultaneously grafted with blue and yellow Phosphors. *J Am Chem Soc* 2012; 134: 20290-3.
- [29] Zhao J, Yu Y, Yang X, Yan X, Zhang H, Xu X, Zhou G, Wu Z, Ren Y, Wong W. Phosphorescent iridium(III) complexes bearing fluorinated aromatic sulfonyl group with nearly unity phosphorescent quantum yields and outstanding electroluminescent properties. *ACS Appl Mater Interfaces* 2015; 7: 24703-14.
- [30] Li Z, Wu Z, Jiao B, Liu P, Wang D, Hou X. Novel 2,4-difluorophenyl-functionalized arylamine as hole-injecting/hole-transporting layers in organic light-emitting devices. *Chem Phys Lett* 2012; 527: 36-41.
- [31] Babudri F, Farinola G, Naso F, Ragni R. Fluorinated organic materials for electronic and optoelectronic applications: the role of the fluorine atom. *Chem Commun* 2007; 1003-22.
- [32] Li Z, Wu Z, Fu W, Liu P, Jiao B, Wang D, Zhou G, Hou X. Versatile fluorinated derivatives of

triphenylamine as hole-transporters and blue-violet emitters in organic light-emitting devices.

J Phys Chem C 2012; 116: 20504-12.

[33] Crosby G, Demas J. Measurement of photoluminescence quantum yields. J Chem Phys 1971; 75: 991-1024.

[34] Zhang H, Wan X, Xue X, Li Y, Yu A, Chen Y. Selective tuning of the HOMO- LUMO gap of carbazole-based donor-acceptor-donor compounds toward different emission colors. Eur J Org Chem 2010; 1681-7.

[35] Lee C, Yang W, Parr R. Development of the colle-salvetti correlation-energy formula into a functional of the electron density. Phys Rev B 1988; 37: 785-9.

[36] Becke A. A new mixing of Hartree-Fock and local density-functional theories. J Chem Phys 1993; 98: 1372-7.

[37] Frisch M, Trucks G, Schlegel H, Scuseria G, Robb M, Cheeseman J. Gaussian 03, Revision B.05. Pittsburgh, PA: Gaussian, Inc.; 2003.

[38] Wolak M, Delcamp J, Landis C, Lane P, Anthony J, Kafafi Z. High-performance organic light-emitting diodes based on dioxolane-substituted pentacene derivatives. Adv Funct Mater 2006; 16: 1943-9.

[39] Liu X, He C, Huang J, Xu J. Highly efficient blue-light-emitting glass-forming molecules based on tetraarylmethane/silane and fluorene: synthesis and thermal, optical, and electrochemical properties. Chem Mater 2005; 17: 434-41.

Scheme and Figure captions

Scheme 1. Synthetic route towards fluorine-containing C-9 fluorene-functionalized anthracene derivatives

Fig. 1. UV-vis absorption of compounds **3a-3c** and **4a-4c** in CH₂Cl₂ solution (1×10^{-6} M)

Fig. 2. Photoluminescence in dichloromethane solvent (a) (1×10^{-6} M) and in solid states (b)

Fig. 3. The curves of cyclic voltammetry for the fluorine-containing compounds **3a-3c** and **4a-4c**

Fig. 4. HOMO and LUMO electronic density distributions of **3a-3c** and **4a-4c**

Fig. 5. Schematic energy level of different layer (a) and EL spectra of six fluorine-containing fluorenyl-anthracene derivatives at 50 mA (b)

Fig. 6. Luminescence-Voltage (V) (a), Current density (I)-voltage (V) (b) and *L-C* (luminance efficiency vs. current density) characteristics (c) for the six fluorine-containing fluorenyl-anthracene derivatives

► Six new fluorine-containing C9-fluorenyl anthracenes linked by a rigid sp^3 -hybridized carbon atoms were synthesized and characterized. ► The effect of fluorine auxochrome at different position in fluorene moiety on photophysical, electrochemical properties and thermal stabilities were investigated. ► The non-doped organic light-emitting diodes (OLEDs) utilizing C9-methylated fluorinated fluorenyl anthracene **4b** as the emitter exhibits deep-blue emissions CIE x, y (0.159, 0.106) with efficiency of 1.31 cd/A and a maximum brightness of 2040 cd/m² at 14 V. ► The introduction of fluorine atom into fluorenyl functionalized anthracene at C2-position (**4b**) could give the excellent electroluminescent performance among the host emitter materials synthesized in this work.